Journal of Applied Mechanics and Technical Physics, Vol. 51, No. 2, pp. 241–248, 2010

VISCOUS DISSIPATION EFFECTS ON HEAT TRANSFER IN FLOW OVER AN INCLINED PLATE

G. Palani and Kwang Yong Kim

UDC 536.24

The effects of viscous dissipation are considered for natural convection flow past a semi-infinite inclined plate with variable surface temperature. Velocity and temperature profiles, skin friction, and rate of heat transfer are obtained. The effects of Grashof and Prandtl numbers, inclination angle, exponent in the wall temperature variation law, and viscous dissipation parameter on the flow are discussed. It is shown that the time required to reach steady states increases with increasing Prandtl number of the fluid. In addition, an increase in the plate temperature due to viscous dissipation was found to lead to a rise in the average skin friction and a decrease in the average Nusselt number.

Key words: *inclined plate, transient flow, Grashof number, skin friction, viscous dissipative effect.*

Introduction. Free convection is widely used in various engineering devices. Two-dimensional free convection flows past a semi-infinite plate have received the attention of many researchers because of their numerous applications in industry. Unsteady natural convection flow past a semi-infinite vertical plate was first solved by Hellums and Churchill [1] using explicit finite difference scheme. Soundalgekar and Ganesan [2] analyzed the problem of transient free convection on an isothermal flat plate by using an implicit finite difference method. Free convection along an inclined plate has received less attention than the cases of vertical and horizontal plates. Kierkus [3] presented a perturbation solution for the problem of natural convection over an isothermal inclined plate. Chen et al. [4] obtained a numerical solution for the problem of natural convection over an inclined plate with a variable surface temperature or heat flux. Ekambavannan and Ganesan [5] solved the problem of unsteady natural convection boundary layer flow over an inclined plate with a variable surface temperature using the Crank–Nicholson implicit finite difference scheme. It should be noted that in [1–5] unsteady free convective flows were studied ignoring heating due to viscous dissipation.

Taking into account viscous dissipative heat included in the energy equation, Gebhart [6] studied free convective flows over a vertical flat plate subject to isothermal and uniform flux surface conditions. Soundalgekar et al. [7] using an implicit finite difference method, performed a finite difference analysis of transient free convective flow of a viscous dissipative fluid past an infinite vertical plate taking into account viscous dissipative heat. Transient free convection flows of a viscous dissipative fluid past a semi-infinite vertical plate using an implicit finite difference scheme was studied by Soundalgekar et al. [8]. Ganesan and Palani [9] investigated transient unsteady viscous dissipative fluid flow past a semi-infinite isothermal inclined plate by a finite difference scheme. The effect of viscous dissipation and pressure stress work in natural convection along a vertical isothermal plate was examined by Pantokratoras [10] by solving the boundary-layer equations by direct numerical simulation without any approximation. Steady laminar boundary-layer flow along a vertical stationary heated plate with the viscous dissipation of the fluid taken into account was studied by Pantokratoras [11] by numerical solution of the boundary-layer equations. Magyari and Rees [12] investigated the effect of viscous dissipation on Darcy free-convection boundary-layer flow over a vertical plate with an exponential temperature distribution in a porous medium, and determined heat-transfer characteristics of self-similar free convection flows analytically and numerically.

Department of Mechanical Engineering, Inha University, Incheon 402-751, Republic of Korea; gpalani32@yahoo.co.in. Translated from Prikladnaya Mekhanika i Tekhnicheskaya Fizika, Vol. 51, No. 2, pp. 116–125, March–April, 2010. Original article submitted April 21, 2009.

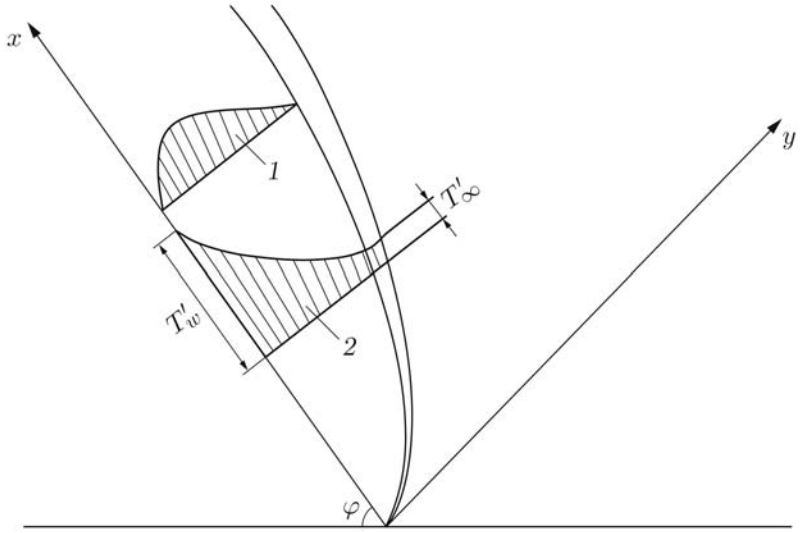

Fig. 1. Flow diagram: 1) hydrodynamic boundary layer; 2) thermal boundary layer.

Viscous dissipation effects may be present in strong gravitational fields and in processes wherein the scale of the process is very large, e.g., on larger planets, in large masses of gas in space, and in geological processes in fluids. As a rule, the heat due to viscous dissipation in the energy equation is very small and can be neglected. However, when the gravitational force or the fluid Prandtl number are very high, the viscous dissipative effects cannot be neglected. Viscous dissipative heat is important even in the case of free convective flows with a high fluid Prandtl number. The objective of the present paper is to study unsteady free convective flow past a semi-infinite inclined plate with variable surface temperature taking into account viscous dissipative heat.

1. Formulation of the Problem. Let us consider two-dimensional unsteady flow of an incompressible viscous fluid flow past a semi-infinite inclined plate with variable surface temperature by taking into consideration the viscous dissipative heat. The analysis is based on the following assumptions: 1) the plate is inclined at an angle φ to the horizontal; 2) the x axis is directed along the plate, and the axis y along the upward normal to the plate; 3) at the time $t' \leqslant 0$ (hereinafter, the quantities with prime are dimensional, and the quantities without prime are nondimensional), it is assumed that the plate and the fluid are at the same temperature, and at $t' > 0$ the temperature of the plate increases suddenly to give rise to free convection flows in the vicinity of the plate; 4) the effect of viscous dissipation is considered in the energy equation; 5) all fluid properties are assumed to be constant except for the density variation with temperature, which is considered only in the body force term. A diagram of the flow is given in Fig. 1 (T'_w is the temperature of the plate, and T'_∞ is the temperature of the fluid far from the plate).

Under the usual Boussinesq approximation, the flow can be shown to be governed by the boundary-layer equations

$$\frac{\partial u}{\partial x} + \frac{\partial v}{\partial y} = 0,$$

$$\frac{\partial u}{\partial t'} + u\,\frac{\partial u}{\partial x} + v\,\frac{\partial u}{\partial y} = g\beta\cos\varphi\,\frac{\partial}{\partial x}\int\limits_y^\infty (T' - T'_\infty)\,dy + g\beta\sin\varphi\,(T' - T'_\infty) + \nu\,\frac{\partial^2 u}{\partial y^2}, \tag{1}$$

$$\frac{\partial T'}{\partial t'} + u\,\frac{\partial T'}{\partial x} + v\,\frac{\partial T'}{\partial y} = \alpha\,\frac{\partial^2 T'}{\partial y^2} + \frac{\mu}{\rho C_p}\Big(\frac{\partial u}{\partial y}\Big)^2$$

with the initial and boundary conditions

$$
\begin{aligned}
&t' \leqslant 0: \quad u = 0, \quad v = 0, \quad T' = T'_\infty && \forall\ y,\\
&t' > 0: \quad u = 0, \quad v = 0, \quad T'_w(x) = T'_\infty + ax^n && \text{at } y = 0,\\
&\qquad\quad u = 0, \quad T' = T'_\infty && \text{at } x = 0,\\
&\qquad\quad u \to 0, \quad T' \to T'_\infty && \text{at } y \to \infty.
\end{aligned} \tag{2}
$$

Here x and y are spatial coordinates along and normal to the plate, respectively, u and v are the velocity components in the x and y directions, respectively, ρ is the density, T' is the temperature, g is the acceleration due to gravity, C_p is the specific heat capacity at constant pressure, β is the coefficient of volumetric thermal expansion, ν is the kinematic viscosity, μ is the dynamic viscosity, a is a constant, n is the exponent in the law of wall-temperature variation, and α is the thermal diffusivity.

We introduce the following nondimensional quantities:

$$
X = \frac{x}{L}, \quad Y = \frac{y}{L}\,\mathrm{Gr}^{1/4}, \quad U = \frac{uL}{\nu}\,\mathrm{Gr}^{-1/2}, \quad V = \frac{vL}{\nu}\,\mathrm{Gr}^{-1/4},
$$

$$
t = \frac{\nu t'}{L^2}\,\mathrm{Gr}^{1/2}, \quad T = \frac{T' - T'_\infty}{T'_w(L) - T'_\infty}, \quad \mathrm{Gr} = \frac{g\beta L^3 (T'_w(L) - T'_\infty)}{\nu^2}, \quad \mathrm{Pr} = \frac{\nu}{\alpha}
$$

(Gr and Pr are the Grashof and Prandtl numbers, respectively, and L is the length of the plate).

The local skin friction τ_x and the average skin friction τ_L are given by the relations

$$
\tau_x = \mu\Big(\frac{\partial u}{\partial y}\Big)\Big|_{y=0}, \qquad \bar{\tau}_L = \frac{1}{L}\int\limits_0^L \mu\Big(\frac{\partial u}{\partial y}\Big)\Big|_{y=0}\,dx,
$$

$$
\mathrm{Nu}_x = -\frac{x}{T'_w - T'_\infty}\Big(\frac{\partial T'}{\partial Y}\Big)\Big|_{y=0}, \qquad \overline{\mathrm{Nu}}_L = -\int\limits_0^L \frac{1}{T'_w - T'_\infty}\Big(\frac{\partial T'}{\partial Y}\Big)\Big|_{y=0}\,dx,
$$

where Nu_x is the local Nusselt number and Nu_L is the average Nusselt number.

Equations (1) and (2) can be written in nondimensional form as

$$
\frac{\partial U}{\partial X} + \frac{\partial V}{\partial Y} = 0,
$$

$$
\frac{\partial U}{\partial t} + U\,\frac{\partial U}{\partial X} + V\,\frac{\partial U}{\partial Y} = \mathrm{Gr}^{-1/4}\cos\varphi\,\frac{\partial}{\partial X}\int\limits_Y^\infty T\,dY + T\sin\varphi + \frac{\partial^2 U}{\partial Y^2}, \tag{3}
$$

$$
\frac{\partial T}{\partial t} + U\,\frac{\partial T}{\partial X} + V\,\frac{\partial T}{\partial Y} = \frac{1}{\mathrm{Pr}}\,\frac{\partial^2 T}{\partial Y^2} + \varepsilon\Big(\frac{\partial U}{\partial Y}\Big)^2,
$$

where $\varepsilon = g\beta L/C_p$ is the viscous dissipation coefficient equal to the kinetic energy of the flow divided by the heat transferred to the fluid. The corresponding initial and boundary conditions in nondimensional form are as follows:

$$
\begin{aligned}
&t \leqslant 0: \quad U = 0, \quad V = 0, \quad T = 0 && \forall\ y,\\
&t > 0: \quad U = 0, \quad V = 0, \quad T = X^n && \text{at } Y = 0,\\
&\qquad\quad U = 0, \quad T = 0 && \text{at } X = 0,\\
&\qquad\quad U \to 0, \quad T \to 0 && \text{at } Y \to \infty.
\end{aligned} \tag{4}
$$

The expressions for the local and average skin friction and Nusselt number are written in nondimensional form as

$$
\tau_X = \mathrm{Gr}^{3/4}\Big(\frac{\partial U}{\partial Y}\Big)\Big|_{Y=0}, \qquad \bar{\tau} = \mathrm{Gr}^{3/4}\int\limits_0^1 \Big(\frac{\partial U}{\partial Y}\Big)\Big|_{Y=0}\,dX,
$$

$$
\mathrm{Nu}_X = -X\,\mathrm{Gr}^{1/4}\Big(\frac{1}{T}\,\frac{\partial T}{\partial Y}\Big)\Big|_{Y=0}, \qquad \overline{\mathrm{Nu}} = -\,\mathrm{Gr}^{1/4}\int\limits_0^1 \Big(\frac{1}{T}\,\frac{\partial T}{\partial Y}\Big)\Big|_{Y=0}\,dX. \tag{5}
$$

2. Numerical Method. The two-dimensional nonlinear unsteady integrodifferential equations (3) in partial derivatives with the initial and boundary conditions (4) were solved using the implicit finite-difference Crank–Nicholson scheme:

$$\frac{U_{i,j}^{k+1}-U_{i-1,j}^{k+1}+U_{i,j}^{k}-U_{i-1,j}^{k}+U_{i,j-1}^{k+1}-U_{i-1,j-1}^{k+1}+U_{i,j-1}^{k}-U_{i-1,j-1}^{k}}{4\Delta X}+\frac{V_{i,j}^{k+1}-V_{i,j-1}^{k+1}+V_{i,j}^{k}-V_{i,j-1}^{k}}{2\Delta Y}=0; \tag{6}$$

$$\frac{U_{i,j}^{k+1}-U_{i,j}^{k}}{\Delta t}+U_{i,j}^{k}\,\frac{U_{i,j}^{k+1}-U_{i-1,j}^{k+1}+U_{i,j}^{k}-U_{i-1,j}^{k}}{2\Delta X}$$

$$+V_{i,j}^{k}\,\frac{U_{i,j+1}^{k+1}-U_{i,j-1}^{k+1}+U_{i,j+1}^{k}-U_{i,j-1}^{k}}{4\Delta Y}=\mathrm{Gr}^{-1/4}\cos\varphi\,\frac{\partial}{\partial X}\int\limits_{Y}^{\infty}T\,dY$$

$$+\sin\varphi\,\frac{1}{2}\,(T_{i,j}^{k+1}+T_{i,j}^{k})+\frac{U_{i,j-1}^{k+1}-2U_{i,j}^{k+1}+U_{i,j+1}^{k+1}+U_{i,j-1}^{k}-2U_{i,j}^{k}+U_{i,j+1}^{k}}{2(\Delta Y)^2}; \tag{7}$$

$$\frac{T_{i,j}^{k+1}-T_{i,j}^{k}}{\Delta t}+U_{i,j}^{k}\,\frac{T_{i,j}^{k+1}-T_{i-1,j}^{k+1}+T_{i,j}^{k}-T_{i-1,j}^{k}}{2\Delta X}+V_{i,j}^{k}\,\frac{T_{i,j+1}^{k+1}-T_{i,j-1}^{k+1}+T_{i,j+1}^{k}-T_{i,j-1}^{k}}{4\Delta Y}$$

$$=\frac{1}{\mathrm{Pr}}\,\frac{T_{i,j-1}^{k+1}-2T_{i,j}^{k+1}+T_{i,j+1}^{k+1}+T_{i,j-1}^{k}-2T_{i,j}^{k}+T_{i,j+1}^{k}}{2(\Delta Y)^2}+\;+\varepsilon\Big(\frac{U_{i,j+1}^{k+1}-U_{i,j-1}^{k+1}+U_{i,j+1}^{k}-U_{i,j-1}^{k}}{4\Delta Y}\Big)^2. \tag{8}$$

Here the subscripts i and j correspond to points of the grid along the x and y axes, respectively, and the superscript k refers to the point of the grid along the t direction.

We now consider the solution of the two-dimensional equation by the Crank–Nicholson method. The region of integration is a rectangle with sides $X_{\max}=1$ and $Y_{\max}=24$, where $Y_{\max}$ corresponds to $Y=\infty$ (this boundary of the region of integration is away from the thermal and hydrodynamic boundary layers). The value $Y=24$ was chosen so as to satisfy the last two boundary conditions in (4). At $t=0$, the values of U, V, and T are known from the initial conditions at all points of the grid. The computations of U, V, and T on the time layer $k+1$ using the values on the previous layer k are carried out as follows. At the internal nodal points of the computation region, the finite difference equation (8) constitutes a tridiagonal system of equations, which is solved by the Thomas algorithm (see [13]). Thus, values of T are calculated at each nodal point on the $(k+1)$th time layer. The values of U on the $(k+1)$th layer are found similarly by substitution of the values of T on the $(k+1)$th time layer into Eq. (7). Thus, the values T and U are known. Finally, using Eqs. (6), we calculate the values of V at each nodal point on the $(k+1)$th time layer. The computations are carried out until a steady state is reached. The steady-state solution is assumed to have been reached when the absolute difference between the values of U and T in two consecutive time steps is less than 10^{-5} at all points of the grid. The following steps of the grid are chosen: $\Delta X=0.05$ and $\Delta Y=0.25$; a time step $\Delta t=0.01$. When the grid steps in each of the X and Y directions and simultaneously in both directions were halved, the results differed in the fourth decimal place.

The derivatives in Eqs. (5) were evaluated using a five-point approximation formula, and the integrals were then evaluated using the Newton–Cotes closed integration formula Hence, the Crank–Nicholson approximation is consistent and unconditionally stable, and, hence, convergent.

3. Calculation Results and Discussion. A comparison of the calculation results with those of Soundalgekaret [8] shows that they are in satisfactory agreement. From the present numerical results, separation of the boundary layer occurs on the initial time level near the leading edge on the inclined plate. But, separation gets moved along the plate up to a certain height from the leading edge in the earlier transient period by the tangential component of the buoyancy force and by the normal component of the buoyancy force which increases near the leading edge. The tangential component of the buoyancy force decreases with decreasing inclination angle. Hence, the separation moves toward the leading edge in the steady state level as the inclination of the plate reduces. This has been observed previously in studies of the problem of steady state natural convection over an inclined plate.

Figures 2 and 3 shows profiles of the transient velocity and temperature, which have a temporal maximum. This phenomenon was observed in studies of the problem of natural convection on a vertical flat plate. As the angle φ increases, the normal component of the buoyancy force, which causes motion of the fluid along the plate,

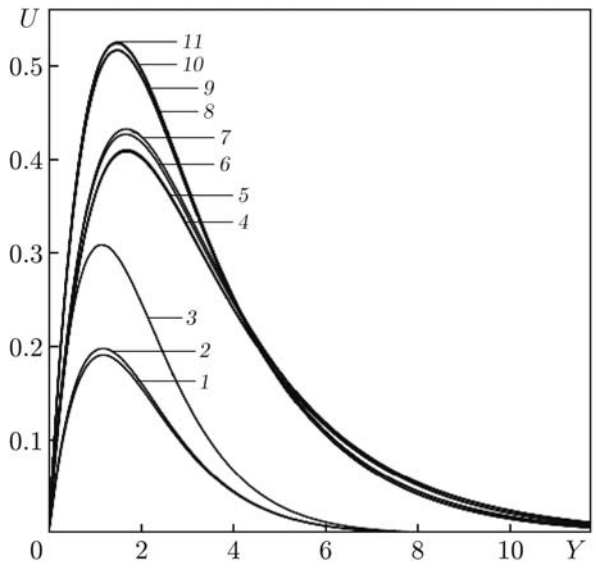

Fig. 2

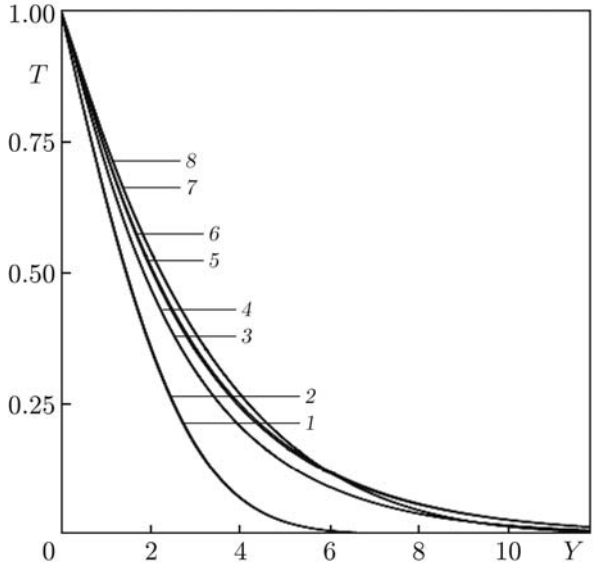

Fig. 3

Fig. 2. Velocity profile of the transient for $X = 1$, Pr $= 0.2$, $n = 1$, $\varepsilon = 1$, and various values of Gr and φ: curves 1 and 2 refer to $\varphi = 30^\circ$, $t = 1$, and Gr $= 10^7$ (1) and 10^6 (2), curve 3 refers to $\varphi = 60^\circ$, $t = 1$, and Gr $= 10^6$, curves 4 and 5 refer to $\varphi = 30^\circ$, Gr $= 10^7$, and $t = 7.64$ (steady state) (4) and $t = 5.62$ (5); curves 6 and 7 refer to $\varphi = 30^\circ$, Gr $= 10^5$, and $t = 7.16$ (steady state) (6) and $t = 5.15$ (7); curves 8 and 9 refer to $\varphi = 60^\circ$, Gr $= 10^7$, and $t = 6.5$ (steady state) (8) and $t = 4.87$ (9), and curves 10 and 11 refer to $\varphi = 60^\circ$, Gr $= 10^6$, and $t = 6.41$ (steady state) (10) and $t = 4.65$ (11).

Fig. 3. Unsteady temperature profiles for $X = 1$, Pr $= 0.2$, $n = 1$, $\varepsilon = 1$ and various values of Gr and φ: curves 1 and 2 refer to Gr $= 10^6$, $t = 0.5$, and $\varphi = 60^\circ$ (1) and 30° (2), curves 3 and 4 refer to $\varphi = 60^\circ$ and Gr $= 10^6$ and $t = 6.41$ (steady state) (curve 3) and Gr $= 10^7$ and $t = 6.5$ (steady state) (curve 4), curves 5 and 6 refer to $\varphi = 30^\circ$ and Gr $= 10^6$ and $t = 7.16$ (steady state) (curve 5) or Gr $= 10^7$ and $t = 7.64$ (steady state) (curve 6), and curves 7 and 8 refer to $\varphi = 30^\circ$ and Gr $= 10^6$ and $t = 2.08$ (curve 7) or Gr $= 10^7$ and $t = 2.1$ (curve 8).

decreases near the leading edge. In this case, the time of establishment of the steady state also decreases. Because, with increasing φ, the tangential buoyancy force dominates downstream and increases, the flow velocity increases.

It is noticed that, with increasing Grashof number, the flow velocity decreases and the temperature increases. In this case, the differences between the maximum velocity and temperature and their values corresponding to the steady state decrease.

The time required for the establishment of the steady state is calculated for various values of the dissipation parameter, parameter n, and fluid Prandtl numbers Pr $= 0.20$, 0.71, 7.00, and 100.00.

Figures 4a and 5b show velocity profiles for the steady state for $X = 1$, $n = 0.5$ and 1.0, $\varepsilon = 1$, 2, and 3, and various values of Pr. It is evident that, for all Prandtl numbers, the steady-state velocity increases with increasing viscous dissipative heating. From Figs. 4a and 5a, it follows that, with increasing Prandtl number, the steady velocity decreases and the time required for the establishment of the steady state increases. Viscous dissipative heating influences the time of establishment of the steady state only for very high fluid Prandtl numbers.

Figures 4b and 5b shows temperature profiles for the steady state for $X = 1$ and various values of the fluid Prandtl number, parameter n, and viscous dissipation parameter ε. It is evident that the temperature increases with increasing viscous dissipative heating, irrespective of the fluid Prandtl number. From Figs. 4b and 5b, it also follows that with the temperature decreases with increasing values of Pr and n.

The local skin friction distribution is shown in Fig. 6. It is evident that the local wall shear stress decreases with increasing Pr because the flow velocity decreases. In addition, with increasing n, the local skin friction decreases because the velocity gradient near the plate decreases (see Fig. 4a). With increasing viscous dissipative heating, the local skin friction increases.

The local Nusselt number distribution is presented in Fig. 7. It is evident that, with increasing n, the Nusselt number increases, but, near the leading edge, it decreases. In addition, the local Nusselt number increases with

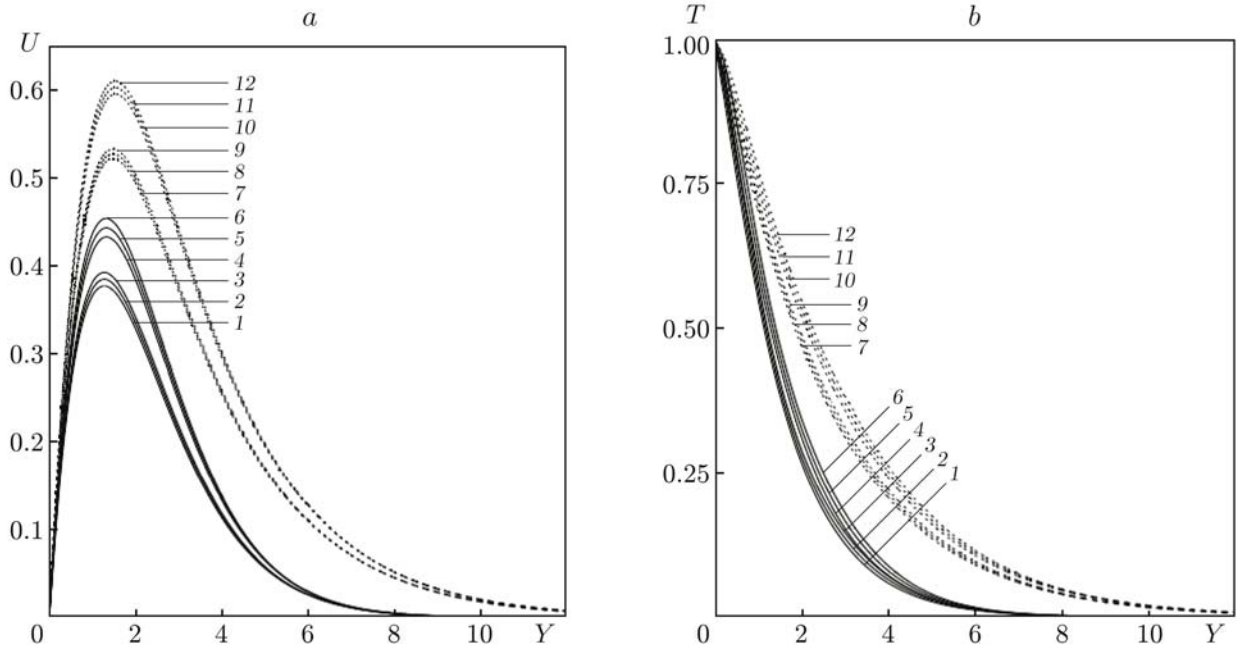

Fig. 4. Velocity profiles (a) and temperature profiles (b) in the steady state for $X = 1$, $\mathrm{Gr} = 10^6$, $\varphi = 60^\circ$, $\mathrm{Pr} = 0.20$ (dotted curves) and 0.71 (solid curves), and $n = 1$ (1–3 and 7–9), 0.5 (4–6 and 10–12): 1) $\varepsilon = 1$ and $t = 6.9$; 2) $\varepsilon = 2$ and $t = 7.02$; 3) $\varepsilon = 3$ and $t = 7.14$; 4) $\varepsilon = 1$ and $t = 5.97$; 5) $\varepsilon = 2$ and $t = 5.99$; 6) $\varepsilon = 3$ and $t = 5.99$; 7) $\varepsilon = 1$ and $t = 6.41$; 8) $\varepsilon = 2$ and $t = 6.4$; 9) $\varepsilon = 3$ and $t = 6.38$; 10) $\varepsilon = 1$ and $t = 5.86$; 11) $\varepsilon = 2$ and $t = 5.83$; 12) $\varepsilon = 3$ and $t = 5.79$.

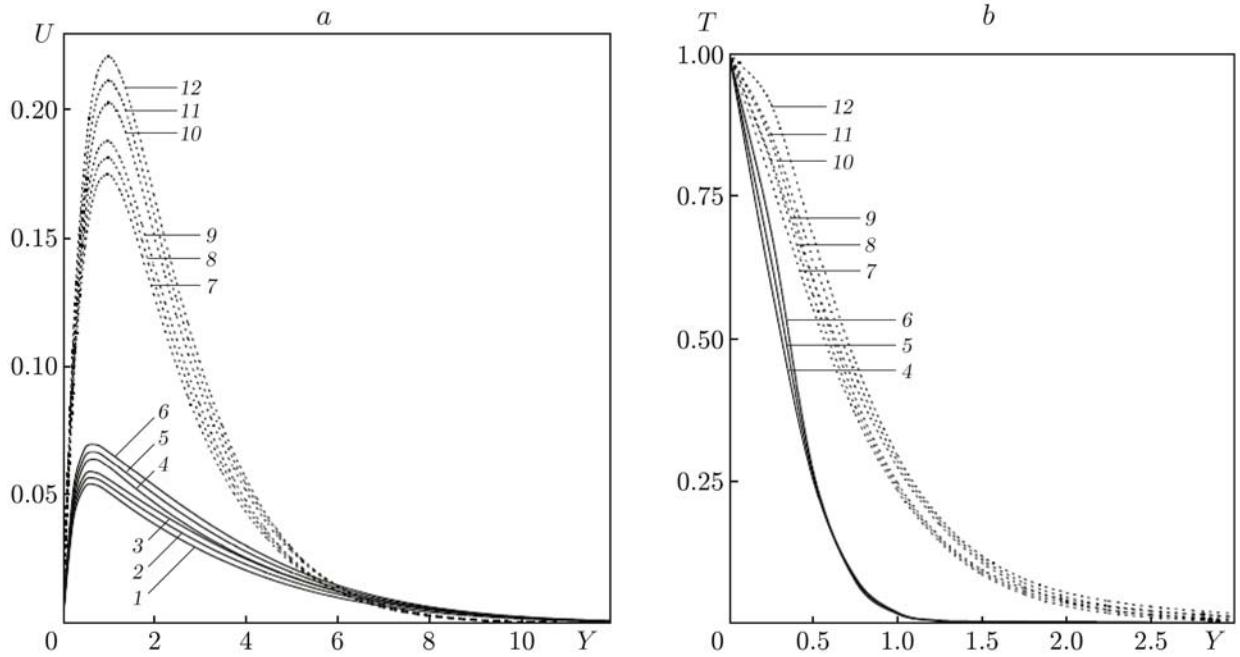

Fig. 5. Velocity profiles (a) and temperature profiles (b) in the steady state for $X = 1$, $\mathrm{Gr} = 10^6$, $\varphi = 60^\circ$, $\mathrm{Pr} = 7$ (dotted curves) and 100 (solid curves), and $n = 1$ (1–3 and 7–9) and 0.5 (4–6 and 10–12): 1) $\varepsilon = 1$ and $t = 19.02$; 2) $\varepsilon = 2$ and $t = 20.9$; 3) $\varepsilon = 3$ and $t = 22.48$; 4) $\varepsilon = 1$ and $t = 18.9$; 5) $\varepsilon = 2$ and $t = 19.86$; 6) $\varepsilon = 3$ and $t = 20.46$; 7) $\varepsilon = 1$ and $t = 10.92$; 8) $\varepsilon = 2$ and $t = 11.14$; 9) $\varepsilon = 3$ and $t = 11.31$; 10) $\varepsilon = 1$ and $t = 10.29$; 11) $\varepsilon = 2$ and $t = 10.42$; 12) $\varepsilon = 3$ and $t = 10.5$.

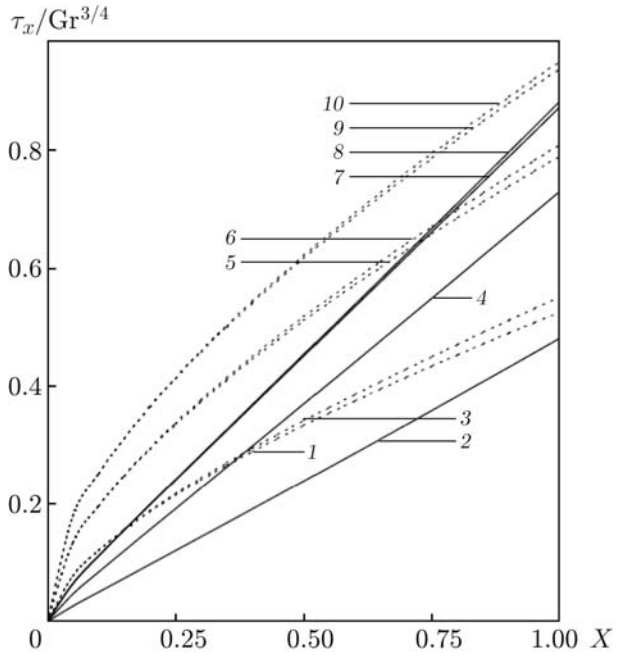

Fig. 6

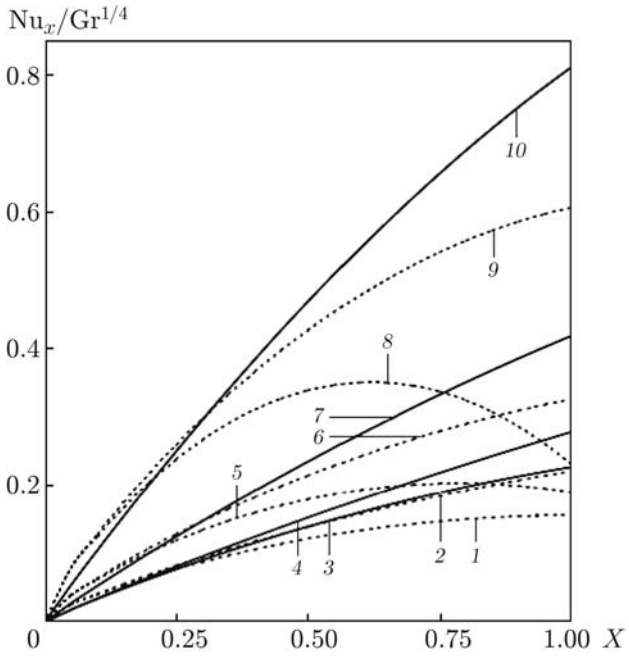

Fig. 7

Fig. 6. Local skin friction distribution over the plate ($\mathrm{Gr} = 10^6$ and $\varphi = 60°$) for $n = 0.5$ (dotted curves) and 1 (solid curves), $\mathrm{Pr} = 7$ (1–3), 0.71 (4–6), and 0.2 (7–10), and $\varepsilon = 1$ (1, 4, 5, 7, and 8) and $\varepsilon = 2$ (2, 3, 6, 9, and 10).

Fig. 7. Distribution of local Nusselt number on the plate ($\mathrm{Gr} = 10^6$ and $\varphi = 60°$) for $n = 0.5$ (dotted curves) and 1 (solid curves), $\mathrm{Pr} = 0.2$ (1–4), 0.71 (5–7), and 7 (8–10), and $\varepsilon = 1$ (3, 4, 6, 7, 9, and 10) and 2 (1, 2, 5, and 8).

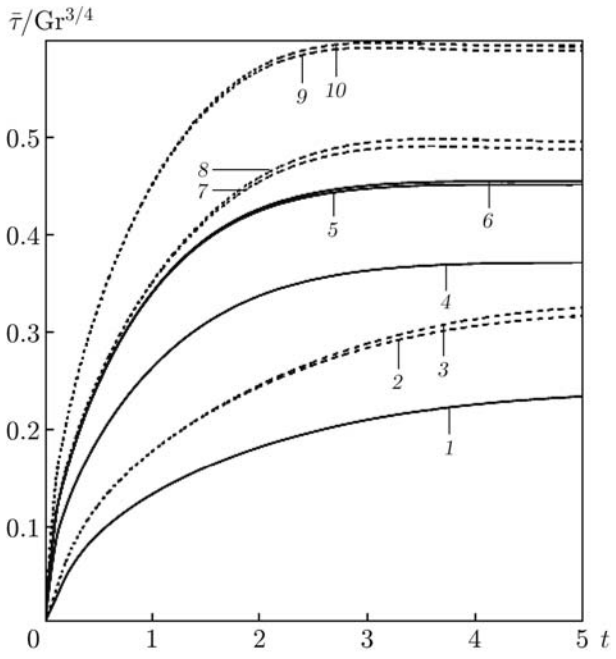

Fig. 8

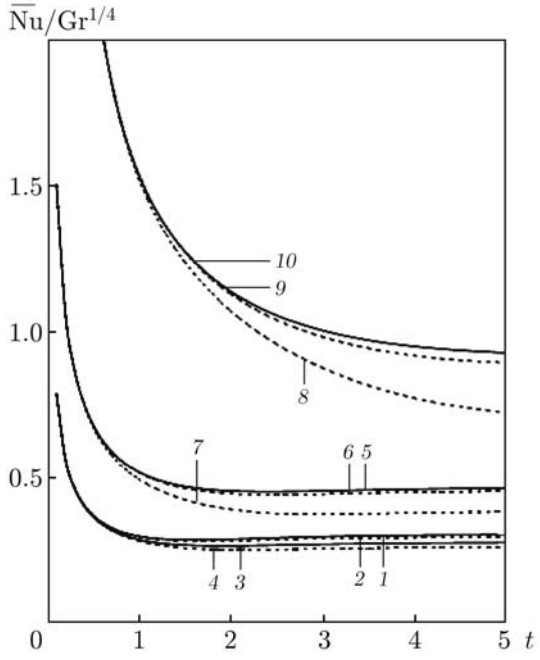

Fig. 9

Fig. 8. Average skin friction distribution over the plate ($\mathrm{Gr} = 10^6$ and $\varphi = 60°$) for $n = 0.5$ (dotted curves) and 1 (solid curves), $\mathrm{Pr} = 7$ (1–3), 0.71 (4, 7, and 8), and 0.2 (5, 6, and 10), and $\varepsilon = 1$ (1, 2, 4, 5, 7, and 9) and 2 (3, 6, 8, and 10).

Fig. 9. Average Nusselt number distribution over the plate ($\mathrm{Gr} = 10^6$ and $\varphi = 60°$) for $n = 0.5$ (dashed curves) and 1 (solid curves), $\mathrm{Pr} = 0.2$ (1–4), 0.71 (5–7), and 7 (8–10), and $\varepsilon = 1$ (1, 2, 5, 6, 9, and 10) and 2 (3, 4, 7, and 8).

increasing Pr . In Fig. 7, it is also evident that an increase in the viscous dissipative heating leads to a reduction in the local Nusselt number.

The average values of the skin friction and Nusselt number are given in Figs. 8 and 9, respectively. The average skin friction decreases with increasing n because the velocity gradient near the plate decreases. The average skin friction increases with time and asymptotically reaches a constant value. An increase in the viscous dissipative heating leads to an increase in the average skin friction. The average skin friction decreases with increasing Prandtl number.

From Fig. 9, it follows that in the initial period, the average Nusselt does not change as n varies. This implies that, initially, heat transfer occurs only by heat conduction. In the initial period of convection, the average Nusselt slightly decreases and then increases with increasing n. From Fig. 9, it also follows that the average Nusselt decreases with increasing viscous dissipation parameter, irrespective of the Prandtl number. In addition, the average Nusselt increases with increasing Pr .

Conclusions. Unsteady natural convective flow over a semi-infinite inclined plate with variable surface temperature was studied taking into account viscous dissipative heating in the energy equation. The differential equations of the flow were transformed to a system of nondimensional equations, which were solved numerically using an implicit finite difference method. The results of the study leads to the following conclusions. The time of establishment of the steady state decreases as the angle φ increases. The difference between the maximum values of the velocity and temperature and the steady-state value, decreases with increasing Grashof number. The steady-state velocity increases with increasing viscous dissipative heat for all Prandtl numbers. An increase in the viscous dissipation heating leads to a rise in the local skin friction, The temperature decreases with greater viscous dissipative heat, irrespective of the fluid Prandtl number. Greater viscous dissipative heating causes a rise in the local skin friction. The average Nusselt number decreases with increasing viscous dissipation parameter, irrespective of the Prandtl number.

REFERENCES

1. J. D. Hellums and S. W. Churchill, "Transient and steady state, free and natural convection, numerical solutions. Part 1. The isothermal vertical plate," *AIChE J.*, **8**, No. 5, 690–692 (1962).
2. V. M. Soundalgekar and P. Ganesan, "Finite difference analysis of transient free convection on an isothermal vertical at plate," *Region. J. Energ. Heat Mass Transfer*, **13**, 219–224 (1981).
3. W. T. Kierkus, "An analysis of laminar free convection flow and heat transfer about an inclined isothermal plate," *Int. J. Heat Mass Transfer.*, **11**, 241–253 (1968).
4. T. S. Chen, H. C. Tien, and B. F. Armaly, "Natural convection on horizontal, inclined and vertical plates with variable surface temperature or heat flux," *Int. J. Heat Mass Transfer.*, **29**, 1465–1478 (1986).
5. K. Ekambavannan and P. Ganesan, "Finite difference solution of unsteady natural convection boundary layer flow over an inclined plate with variable surface temperature," *Wärme-und Stoffübertrag*, **30**, 63–69 (1994).
6. B. Gebhart, "Effects of viscous dissipation in natural convection," *J. Fluid Mech.*, **14**, 225–232 (1962).
7. V. M. Soundalgekar, R. M. Lahurikar, and S. G. Pohanerkar, "Transient free convection flow of an incompressible viscous dissipative fluid," *Heat Mass Transfer.*, **32**, No. 4, 301–305 (1997).
8. V. M. Soundalgekar, B. S. Jaiswal, A. G. Uplekar, and H. S. Takhar, "Transient free convection flow of viscous dissipative fluid past a semi-infinite vertical plate," *J. Appl. Mech. Eng.*, **4**, No. 2, 203–218 (1999).
9. P. Ganesan and G. Palani, "Transient free convection flow of viscous dissipative fluid past a semi-infinite inclined plate," *J. Appl. Mech. Eng.*, **8**, No. 3, 395–402 (2003).
10. A. Pantokratoras, "Effect of viscous dissipation and pressure stress work in natural convection along a vertical isothermal plate. New results," *Int. J. Heat Mass Transfer*, **46**, 4979–4983 (2003).
11. A. Pantokratoras, "Effect of viscous dissipation in natural convection along a heated vertical plate," *Appl. Math. Modelling*, **29**, 553–564 (2005).
12. E. Magyari and D. A. S. Rees, "Effect of viscous dissipation on the Darcy free convection boundary-layer flow over a vertical plate with exponential temperature distribution in a porous medium," *Fluid Dyn. Res.*, **38**, 405–429 (2006).
13. B. Carnahan, H. A. Luther, and J. O. Wilkes, *Applied Numerical Methods*, John Wiley and Sons, New York (1969).